



## Multiscale FE-Studies of Contact Stresses of Dry and Lubricated Shot Peened Workpiece Surfaces

Fritz Klocke<sup>1</sup>, Daniel Trauth<sup>\*1</sup>, Patrick Mattfeld<sup>1</sup>, Anton Shirobokov<sup>1</sup>, Kirsten Bobzin<sup>2</sup>, Tobias Brögelmann<sup>2</sup>, Serhan Bastürk<sup>2</sup>

<sup>1</sup>Laboratory for Machine Tools and Production Engineering (WZL), RWTH Aachen University, Steinbachstr. 19, 52074 Aachen, Germany

<sup>2</sup>Surface Engineering Institute (IOT), RWTH Aachen University, Kackertstr. 15, 52072 Aachen, Germany

### Abstract

In production engineering cold forging processes are of great importance due to the high material utilization and the associated energy and resource efficiency. In order to perform cold forging processes successfully, liquid and solid lubricants are used, which are often questionable due to ecological, economic, and legislative reasons. For these reasons, dry metal forming exhibits an increased research potential. The absence of lubricants in dry metal forming contributes significantly to the waste reduction in manufacturing processes and to the goal of a lubricant-free factory. However, the abdication of lubricants goes along with the requirement that the dry tribological system has to withstand the increased tribological loads. In this contribution an empirical approach to meet the challenges in dry metal forming is proposed. Shot peened surface structures on workpieces are numerically investigated in order to identify friction and, thus, tool-load reducing surfaces compared with non-structured workpieces. In future work, this approach will be synthesized with a (Cr,Al)N PVD-tool-coating with self-lubricating disulfides to achieve a lubricant free cold forging.

**Keywords:** Dry metal forming, Coating, HPPMS, (Cr,Al)N, Surface structures, Pin-On-Cylinder Tribometer

### 1 Introduction

In production engineering cold forging processes are of great importance due to the high material utilization and the associated energy and resource efficiency [1]. Cold forged parts are typically used within the drive technology, e.g. as driving shafts. In order to perform cold forging processes successfully, liquid and solid lubricants are used, which may be questionable due to ecological, economic, and legislative reasons [2]. Research is reducing these factors by using biodegradable lubricants and hard coatings. Lugscheider et al. developed a (Ti,Hf,Cr)N PVD-coating for cold metal forming applications within the collaborative research center ‘Environmentally friendly tribological systems’ [3]. A development of a special tool coating with self-lubricating disulfides for dry metal forming will be performed on top in the future. As a further step, the complete absence of lubricants is the focus of many ongoing projects in dry metal forming which contributes significantly to the waste reduction in manufacturing processes and to the goal of a lubricant-free factory [4]. The first steps in this

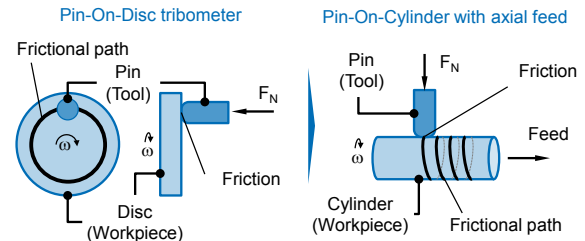
area were taken by Murakawa et al., who successfully performed dry sheet metal forming operations of aluminum using diamond-like-carbon coatings [5,6]. Their research was extended by Osakada et al. who investigated the impact of surface roughness on the coefficient of friction [7]. Kataoka et al. [8,9] and Tamaoki et al. [10,11] investigated dry deep drawing with ceramic tools and achieved comparable results with the lubricated forming of low-alloyed steels, stainless steels, and aluminum. The state of the art mainly covers sheet metal forming processes, but reveals the potential of tool coatings to withstand the tool loads in dry metal forming. Especially, (Cr,Al)N is a promising candidate for forming applications [12] due to its high hardness and good abrasion resistance [13]. Compared with sheet metal forming cold forging is characterized by higher contact pressures and surface expansion of the workpiece [14]. Therefore, the abdication of lubricants goes along with the requirement that the dry tribological system has to withstand the increased tribological loads [15]. The overall approach is shown in Fig. 1. On the one hand, the influence of

The diagram illustrates a tribosystem for dry metal forming. It shows a cross-section of the tool, interface, coating, matrix, and disulfide layers. The tool is labeled "Tool" and the workpiece is labeled "Workpiece". The interface is labeled "Interface". The coating is labeled "Coating". The matrix is labeled "Matrix". The disulfide layer is labeled "Disulfide". The workpiece surface is labeled "Surface topography". The workpiece is labeled "Workpiece". The workpiece is labeled "Workpiece". The workpiece is labeled "Workpiece".

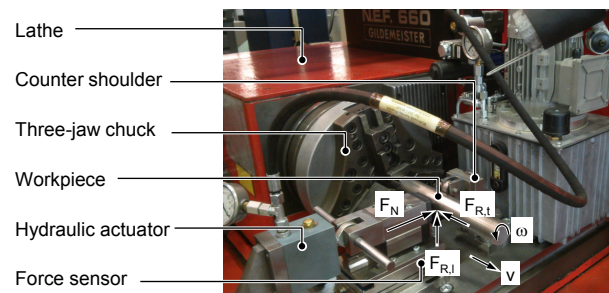
The approach pursued in this paper is based on two main steps. The advances in surface structures on workpieces are investigated to provide friction reducing surfaces in dry metal forming. Firstly, a novel Pin-On-Cylinder (POC) tribometer with axial feed is presented in section 2.1. This POC tribometer allows the investigation of surface smoothing effects and, thus, surface structures for the first time. Afterwards, numerical studies of dry and lubricated contacts of shot peened surfaces using finite element method (FEM) are performed to provide fundamental insights, see Section 2.2. Future work will cover experimental studies of the influences of shot peened surfaces on friction force and frictional shear stresses using the POC tribometer. Concluding, the scientific findings are summarized and an outlook for future investigations is given in the last Section 3.

This section describes the development of a novel Pin-On-Cylinder tribometer with axial feed. This is necessary as existing tribometers (e.g. Pin-On-Disc) do not allow for the investigation of surface smoothing effects. They usually use the same friction path each revolution. This results in different contact conditions per revolution and prohibits investigating the influence of surface structures. Afterwards, numerical studies using FEM are performed to provide hardly measurable insights within the contact zone in POC tribotesting of shot peened surfaces.

Figure 2 illustrates the disadvantage of conventional Pin-On-Disc (POD) tribometers when analyzing the effect of surface structures is of main concern.



The developed Pin-On-Cylinder (POC) tribometer was designed to allow an investigation of surface structures during a certain time period. The POC prototype is mounted on the sliding carriage of a lathe, see Fig. 3. Workpiece clamping and rotation as well as the machine feed are performed by the lathe. The normal load which presses the pin on the workpiece is applied by a hydraulic actuator. This tribometer design enables a continuous investigation of surface effects along the frictional path.



In order to understand the frictional mechanisms in tribotesting, numerical studies are performed to analyze globally the contact stresses and locally occurring surface smoothing effects.

The numerical investigations are separated into two modeling approaches, see Fig. 4. Firstly, a macro simulation determining the global contact stresses and true strains is performed. In the macro simulation surface roughness and surface structures are neglected due to numerical reasons. Afterwards, a micro simulation is set-up. The micro simulation only covers a small cut-out of the workpiece, but takes into account the smoothing of a surface topography of a real shot peened surface. The global stresses from the macro simulation are mapped onto the lateral surfaces of the cut-out model to provide a realistic material behavior.

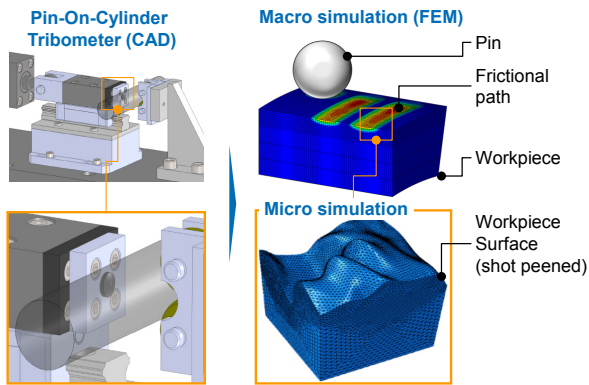


Figure 4: Modeling of the macroscopic tribometer contact and the microscopic interactions using dry and lubricated shot peened surfaces.

### 2.2.1 Macro simulation of contact stresses in POC tribotesting

The aim of the macro model is to provide two fundamental informations about tribotesting using the POC tribometer. Firstly, the critical feed per revolution must be known to avoid interferences of advanced frictional paths. This is necessary to reduce the experimental effort in the experimental tribotests in the future. Secondly, true strains, contact stresses, contact areas, and indentation depths of the frictional paths have to be determined to provide fundamental insights.

Macro modeling was performed explicitly in Abaqus 6.13-1. The workpiece was modeled elasto-plastically. Material characteristics for the workpiece material 16MnCr5 (DIN: 1.7131, AISI: 5115) were determined in preliminary work [15]. The deformable workpiece was modeled in 3D using hexagonal continuum elements with reduced integration (C3D8R). A fine mesh (axial, radial, and tangential seed of 100  $\mu\text{m}$ ) ensures a high resolution of the investigated surface layer to a depth of 0.5 mm. Process kinematics of the Pin was performed by means of a bushing connector according to [16]. The normal force  $F_N$  was varied between 0.5 kN and 10 kN. Figure 5 shows the results. A nearly linear correlation between normal force  $F_N$  and critical feed  $f_{\text{crit}}$  with a slightly degressive characteristics is found. This allows a numerical and experimental investigation of non-influencing frictional paths.

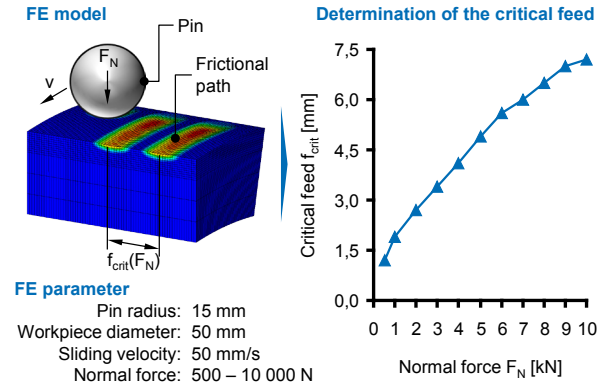


Figure 5: Set-up of the macroscopic FE model and determination of the critical feed.

Analysis of true strains, contact stresses, contact area, and indentation depths of the frictional paths were performed with the presented FE model simulating only one path. Figure 6 shows that the true strain increases significantly up to  $\phi_v = 1.8$  with increasing normal force  $F_N$ . This corresponds to an intensive strain hardening, which either leads to surface fatigue or increases significantly the tool loads in dry metal forming due to the surface hardening. Further, the simulations show, that indentation depths up to  $\Delta h = 35 \mu\text{m}$  occur.

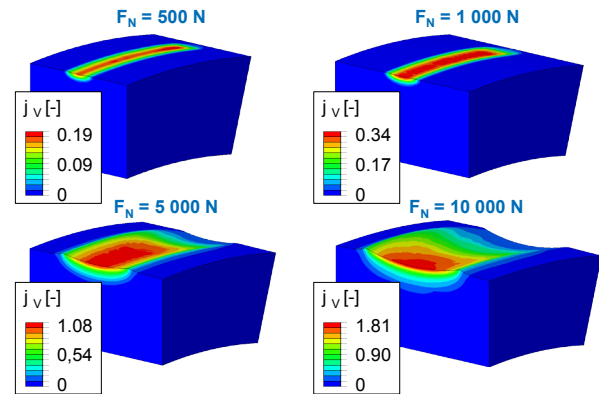


Figure 6: Analysis of the true strains along the frictional path. Legend:  $\phi_v$  = true strain.

In Fig. 7 the contact area and contact stresses during tribotesting are shown. It is observed that the contact area is approximately half a spherical dome area. Additionally, the contact stresses are assumed to be of constant magnitude along the semi-axis  $x$ , as the curve characteristics indicates. The irregularities in the curves are due to numerical instabilities and may be neglected.



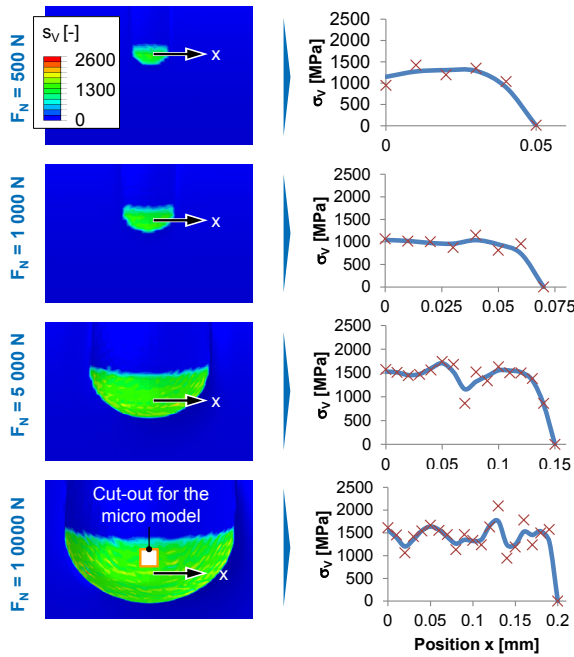


Figure 7: Analysis of the contact stresses along the contact area of a frictional path. Legend:  $\sigma_v$  = contact stresses.

After the simulation of the macroscopic loads, the calculated stresses are mapped to a micro model taking into account the surface topography after shot peening.

### 2.2.2 Micro simulation of dry and lubricated shot peened surfaces

The micro modeling approach is shown in Fig. 8. An experimentally shot peened surface (Fig. 8a) is topographically measured using a combined roughness and contour measurement system Hommel Etamic nanoscan 855 made by Jenoptik AG, Germany. The measurement grid size was  $2 \times 2 \text{ mm}^2$ . A contact tip with a tip angle of  $60^\circ$  and a tip radius of  $2 \text{ }\mu\text{m}$  was used. The evaluated data is shown in Fig. 8b.

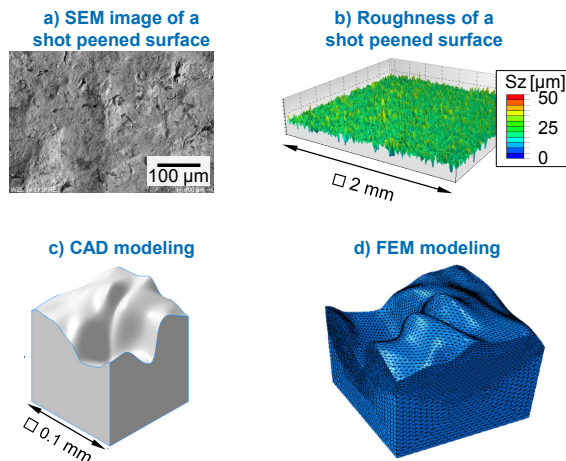


Figure 8: Illustration of the micro modeling approach. A shot peened surface (a) was transferred to a set of data points (b) by tactile measurement. The data point are converted to a three-dimensionally CAD-part (c) and copied to the FE application (d).

Selected data points for a cut out area were afterwards transferred to the CAD modeling tool Catia V5R20. From the data points parallel splines were created. The splines were then lofted to a surface of  $0.1$

$\times 0.1 \text{ mm}^2$  and extruded to build a three-dimensional body (Fig 8c). This approach allows the modeling of solid rather than shell bodies. Solids allow for the mapping of the previously simulated macroscopic stresses onto the FE model. The FE model is shown in Fig 8d.

The material characteristics are identical to the macro model. Meshing was performed with four-node tetrahedral elements to respect the complex surface topography. The fine mesh seed near the surface was set to  $1.5 \text{ }\mu\text{m}$ . The base body was seeded with  $5 \text{ }\mu\text{m}$ . Process kinematics differ from the macro model. Only a normal contact is modelled. The normal contact is carried out by a displacement of a rigid planar body. The displacement was set to the maximum of the previously determined indentation depth of  $\Delta h = 35 \text{ }\mu\text{m}$ . The stresses from the macro model are mapped onto the micro model by the Abaqus option *predefined fields*.

Surface smoothing of the micro model was further distinguished in dry and lubricated modeling. This allows the distinct analysis and comparison of smoothing effects in dry and lubricated contacts. The lubricant was modeled as an Euler part using the Coupled-Eulerian-Lagrangian (CEL) approach. The mesh size of the Euler part was accordingly set to  $1.5 \text{ }\mu\text{m}$  as the surface. As lubricant an incompressible mineral oil with a density of  $\rho = 1.01 \text{ g/cm}^3$  and dynamic viscosity of  $\eta = 230 \text{ mPa s}$  was defined. Figure 9 shows the surface smoothing of a shot peened surface at three distinct smoothing positions. It is observed that a fluid pressure up to  $p_{FL} = 300 \text{ MPa}$  is build-up in the lubricant.

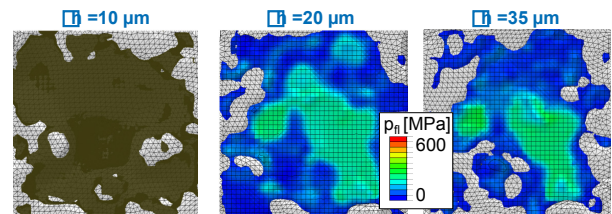


Figure 9: Smoothing of a shot peened surface with lubricant.

In lubricated contacts, this fluid pressure is very beneficial as it supports the tribosystems by providing a supporting lubricant reservoir. However, as lubricants are assumed to be incompressible in technological applications, it prevents the workpiece surface to smoothen completely. Therefore, the true contact area remains smaller than theoretically possible.

In Fig. 10 the influence of smoothing of dry and lubricated contacts is analyzed by comparison of the contact area. It is observed that already after a smoothing of  $10 \text{ }\mu\text{m}$  the investigated structure valley in dry metal forming is significantly smaller than in lubricated contacts. This is due to the incompressible lubricant which prevents the structure valley to deform plastically. At the end of the smoothing at  $\Delta h = 35 \text{ }\mu\text{m}$  the structure valleys are almost completely evened out in dry metal forming. Thus, leading to a significantly increased contact area compared with the lubricated contact.

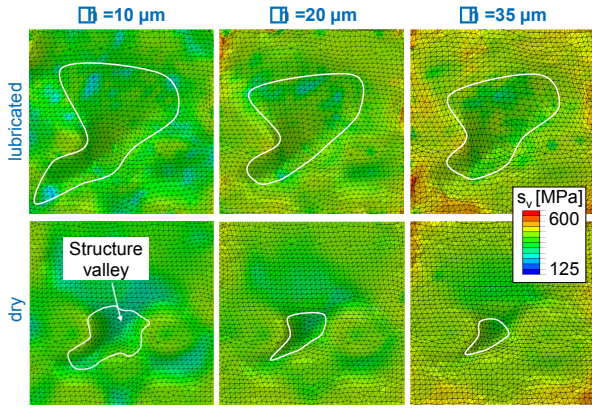


Figure 10: Comparison of the true contact area during smoothing in dry and lubricated forming.

An increased and especially dry true contact area might lead to an increased chemically induced friction, however, the mechanical stresses are clearly smaller due to the increased area. By these means the coating will be exposed to lower contact stresses ensuring its adhesive strength. At the same time the negative effect of chemically induced friction will be mitigated by the coating itself. From further simulations the following model is derived.

### 2.3 Discussion

Figure 11 illustrates a simplified surface structure in dry and lubricated forming. The simplified contact situation serves as a basis for the analytical explanation of the observed phenomena, that contact stresses in dry metal forming are reduced from mechanical point of view compared with lubricated situations. In lubricated contacts hydrostatic fluid pressures reach up to  $p_{FL} = 300$  MPa. These fluid pressures support the tribosystem but also reduce the true contact area as they prevent the surface to even out.

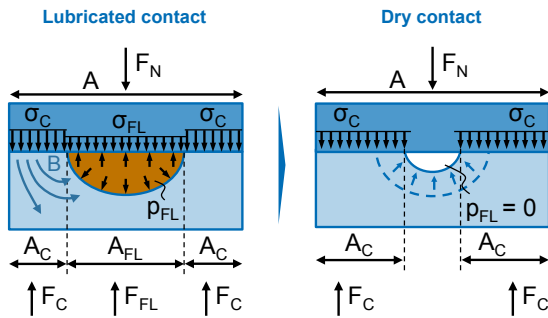


Figure 112: Model of contact stresses in dry metal forming of surface structured compared with lubricated contacts

From Fig. 11 it is assumed, that an external normal force  $F_N$  applied by a tool evokes reaction forces in the fluid ( $F_{FL}$ ) as well as in the hard contact ( $F_C$ ), see Eq. 1:

$$F_N = 2 F_C + F_{FL}. \quad (1)$$

Therefore, the contact force is derived to be, see Eq. 2:

$$F_C = \frac{1}{2} (F_N - F_{FL}). \quad (2)$$

Related to the different contact areas, the resulting contact stress  $\sigma_C$  is, see Eq. 3:

$$\sigma_C = \frac{1}{2} \left( \frac{F_N}{A_C} - p_{FL} \left( \frac{A}{A_C} - 2 \right) \right). \quad (3)$$

From Eq. 3 it is concluded that contact stresses increase proportionally with the external load  $F_N$ , but also with reducing contact areas  $A_C$ . In lubricated contacts this means that there is a trade-off between fluid pressure and true contact area. In dry contacts, as  $p_{FL} = 0$ , contact stresses depend only on the true contact area. As this true contact area increases due to a material deformation, contact stresses might be decreased compared with lubricated contacts, if the trade-off between fluid pressure and true contact area is not adjusted properly. From Eq. 3 it is also concluded, that smooth surfaces structures lead to the lowest contact stresses as they have the highest true contact area. Therefore, surface structure achieved by shot peening might be disadvantageous in dry forming. However, a tribological system is not only characterized by mechanical loads but also by thermo-chemical interactions between tool and workpiece. Thus, experimental test using the developed POC tribometer will proof, if surface structures are beneficial regarding thermal and chemical effects.

### 3 Conclusion and outlook

The absence of lubricants in dry metal forming significantly contributes to the waste reduction in manufacturing processes and to the goal of a lubricant-free factory. However, the abdication of lubricants goes along with the requirement that the dry tribological system has to withstand the increased tribological loads. In this contribution, an empirical approach to meet the challenges in dry metal forming is proposed.

In general, the WZL focusses on surface structures on workpieces by shot peening in order to experimentally study and characterize the influence of the surface structures on the thermo-mechanical-chemical effects. To experimentally do so, a novel Pin-On-Cylinder tribometer with axial feed was developed and presented in this work. This tribometer allows for the investigation of surface smoothing effects and, thus, surface structures for the first time. This is necessary as existing tribometers mostly use the same frictional path per revolution. Afterwards, the stresses and strains in this tribo contact were numerically investigated using the finite element method. A macroscopic FE model was set-up to analyze the global stresses and strains induced in the tribological contact neglecting the surface topography. Afterwards, the global stresses were mapped onto a micro model taking the surface topography of a real shot peened surface into account. Micro modeling was performed for dry and lubricated contacts to analyze and compare the effect of surface smoothing dependent on the fluid pressure and (dry) contact areas. Due to the incompressibility of the lubricant the true contact area between tool and workpiece in lubricated tribosystems is smaller compared to dry contacts. Therefore, the contact stresses are mechanically higher in lubricated as in dry contacts. However, contact stresses in lubricated contacts depend on a trade-off between the contact area

and the induced fluid pressure. Thus, if properly designed, lubricated tribosystems outperform dry contacts.

In the future, tribological tests using the novel Pin-On-Cylinder tribometer will be performed to experimentally analyze the friction force and the frictional shear stress dependent on various shot peened surfaces. The tribological tests will be performed dry und lubricated. Additionally, the pins will be coated with the self-lubricating HPPMS coating analyzing (Cr,Al)N-matrices differently mixed with disulfides.

## Acknowledgements

The research was funded by the German Research Foundation (Deutsche Forschungsgemeinschaft DFG) within the priority program „Dry metal forming – sustainable production through dry processing in metal forming (Trockenumformen – Nachhaltige Produktion durch Trockenbearbeitung in der Umformtechnik (SPP 1676)). Further the authors thank Stefan Ossenkemper from the Institute of Forming Technology and Lightweight Construction for his inspiring preliminary work.

## References

- [1] F. Klocke: Manufacturing processes 4 – Forming, Springer, (2013).
- [2] H. Czichos, K. H. Habig: Tribologie-Handbuch. Tribometrie, Tribomaterialien, Tribotechnik. Springer, (2010).
- [3] E. Lugscheider, K. Bobzin, C. Pinero, F. Klocke, T. Massmann: Development of a superlattice (Ti,Hf,Cr)N coating for cold metal forming applications. Surface and Coatings Technology, 177-178 (2004) 616-622.
- [4] F. Vollertsen, F. Schmidt: Dry Metal Forming: Definition, Chances and Challenges. Int. J. Precision Engineering and Manufacturing – Green Technology 1/1 (2014) 59–62.
- [5] M. Murakawa, N. Koga, T. Kumagai: Deep-drawing of aluminum sheets without lubricant by use of diamond-like carbon coated dies. Surf Coat Tech 76 (1995) 553–558.
- [6] M. Murakawa, S. Takeuchi: Evaluation of tribological properties of DLC films used in sheet forming of aluminum sheet. Surf Coat Tech 163 (2003) 561–565.
- [7] K. Osakada R. Matsumoto: Fundamental Study of Dry Metal Forming with Coated Tools. CIRP Ann. Manuf. Technol 49/1 (2000) 161–164.
- [8] S. Kataoka, A. Motoi. Improvement in DLC thin film adhesion and its application to dry deep drawing. J. Jpn. Soc. Technol. Plast 46/532 (2005) 412–416.
- [9] S. Kataoka, M. Murakawa, T. Aizawa, H. Ike: Tribology of dry deep-drawing of various metal sheets with use of ceramics tools. Surf Coat Tech 177–178 (2004) 582–590.
- [10] K. Tamaoki, S. Kataoka: Study of deep drawing using diamond coated tools. Journal of Material Testing Research Assoc. of Japan 53/4 (2008) 247–253.
- [11] K. Tamaoki, S. Kataoka, K. Minamoto: Dry deep-drawing with use of electroconductive ceramic tools. Proc. Int. Conf. Trib. Manuf. Pro (2007) 175–179.
- [12] J. Lin, B. Mishra, J.J. Moore, W.D. Sproul: Microstructure, mechanical and tribological properties of  $\text{Cr}_{1-x}\text{Al}_x\text{N}$  films deposited by pulsed-closed field unbalanced magnetron sputtering (P-CFUBMS). Surface and Coatings Technology, 201 (2006), 4329.
- [13] N. Bay, A. Azushima: Environmentally benign tribo-systems for metal forming. CIRP Ann. Manuf. Technol. 59/2 (2010) 760–780.
- [14] A. Bruzzzone, H. Costa, P. Lonardo, D. Lucca: Advances in engineered surfaces for functional performance. CIRP Ann. Manuf. Technol. 57 (2008) 750–769.
- [15] P. Mattfeld: Tribologie der zinkphosphatfreien Kaltmassivumformung. PhD-Thesis RWTH Aachen University (2014).
- [16] D. Trauth, F. Klocke, P. Mattfeld, A. Klink: Time-Efficient Prediction of the Surface Layer State after Deep Rolling using Similarity Mechanics Approach. Procedia CIRP 9 (2013) 29–34.